



HAL
open science

Quantification of tributaries contributions using a confluence-based sediment fingerprinting approach in the Canche river watershed (France)

Edouard Patault, Claire Alary, Christine Franke, Nor-Edine Abriak

► **To cite this version:**

Edouard Patault, Claire Alary, Christine Franke, Nor-Edine Abriak. Quantification of tributaries contributions using a confluence-based sediment fingerprinting approach in the Canche river watershed (France). *Science of the Total Environment*, 2019, 668, pp.457-469. 10.1016/j.scitotenv.2019.02.458 . hal-02062245

HAL Id: hal-02062245

<https://hal.science/hal-02062245>

Submitted on 22 Oct 2021

HAL is a multi-disciplinary open access archive for the deposit and dissemination of scientific research documents, whether they are published or not. The documents may come from teaching and research institutions in France or abroad, or from public or private research centers.

L'archive ouverte pluridisciplinaire **HAL**, est destinée au dépôt et à la diffusion de documents scientifiques de niveau recherche, publiés ou non, émanant des établissements d'enseignement et de recherche français ou étrangers, des laboratoires publics ou privés.



Distributed under a Creative Commons Attribution - NonCommercial 4.0 International License

Quantification of tributaries contributions using a confluence-based sediment fingerprinting approach in the Canche river watershed (France).

Edouard Patault^{a,b,*}, Claire Alary^a, Christine Franke^b, Nor-Edine Abriak^a

^aIMT Lille Douai, Univ. Lille, EA 4515 - LGCgE - Civil Engineering and Environmental Department, F-59000 Lille, France

^bMINES ParisTech, PSL Research University, Center of Geosciences, 35 rue Saint-Honoré, 77305 Fontainebleau Cedex, France

**Now at: Normandie Univ, Rouen, UNIROUEN, UNICAEN, CNRS, M2C, FED-SCALE, Rouen, France*

E-mail address: edouard.patault@imt-lille-douai.fr / edouard.patault1@univ-rouen.fr (E.Patault)

Abstract

Since a few years, land use management aims to reduce and control water erosion processes in watersheds but there is a lack of quantitative information on the contribution of the sources of transported sediment. This is most important in agricultural areas where soils are sensitive to erosion. The geology of these areas is often characterized by large expanses of relatively homogeneous quaternary silts. The possibility of distinguishing the sources of erosion according to their geological substratum is thus very delicate. This information is important because its lack can lead to the mis-implementation of erosion control measures. To address this request, a confluence-based sediment fingerprinting approach was developed on the Canche river watershed (1274 km²; northern France), located in the European loess belt, an area that is affected by diffuse and concentrate erosion processes. Suspended particulate matter was collected during five seasonal sampling campaigns using sediment traps at the outlet of each tributary and confluence with the main stream of the Canche river. The final composite fingerprint was defined using physico-chemical and statistical analyses. The best tracer parameters for each tributary were selected using stepwise discriminant function analyses. These parameters were introduced into a mass balance mixing model incorporating Monte-Carlo simulations to represent the uncertainty. Estimates of the overall mean contributions from each tributary were quantified at different temporal scales. The annual sediment flux tributaries contributions range from 3 to 22% at the outlet of the Canche river, and annual sediment flux range from 0.87 to 40.7 kt yr⁻¹. The Planquette and the Créquoise tributaries appear to be those producing the largest sediment flux. In contrast, tributaries with the highest number of erosion control on their area exhibit the lowest values of sediment flux. Our results indicate a positive impact of recent land management policies in the Canche river watershed.

Keywords: sediment fingerprinting; physico-chemical tracers; tributaries; mixing model; watershed management; Northern France

1 **1. Introduction**

2 Information on the origin of sediment transfer in river systems is essential for watershed
3 management. This is a complex task considering that suspended material may come from different
4 diffuse sources and their contribution may vary over time and space as a consequence of varying
5 erosion processes (Haddadchi et al., 2013). Indirect approaches exist to identify sediment sources
6 (field surveys, river monitoring) but they are hampered by spatial and temporal sampling problems
7 (Collins & Walling, 2002). Since several years, direct approaches such as the “sediment
8 fingerprinting” method (e.g. Walling & Woodward, 1992; Collins et al., 2001; Krein et al., 2003;
9 Motha et al., 2004; Martínez-Carreras et al., 2010; Evrard et al., 2011; Lamba et al., 2015) have been
10 commonly applied. These approaches attempt to quantify the contributions of sediment sources at
11 variable spatial scales: from the river section to the catchment scale. The procedure consists on the
12 characterization of the potential sediment sources by a comparison of their bio-geo-physico-chemical
13 properties to the transported fluvial material. The properties that have been used in previous
14 research include sediment color (e.g. Krein et al., 2003; Poulenard et al., 2009; Martínez-Carreras et
15 al., 2010), magnetic properties (e.g. Russell et al., 2001; Motha et al., 2004), chemical composition
16 (e.g. Collins et al., 1997; Carter et al., 2003; Collins et al., 2012; Theuring et al., 2015), environmental
17 radionuclides (e.g. Evrard et al., 2013; Du & Walling, 2016; Le Gall et al., 2016), and particle size (e.g.
18 Krein et al., 2003).

19 There is a consensus that the use of a single parameter is not sufficient, and that a
20 combination of tracers must be used to identify sediment sources (Walling et al., 1993; Collins and
21 Walling, 2002). Because of the heterogeneity of catchments, a large panel of tracers and statistical
22 methods to identify the best combination of parameters that discriminates the sediment sources are
23 generally used (e.g. Collins et al., 1997; Collins et al., 2012; Palazón et al., 2015; Nosrati et al., 2018).
24 Selected data is injected in a mixing model to quantify the contribution of each source to the target
25 sediment. The literature describes different mathematical form of mixing models: e.g. the modified
26 Collins model algorithm, the Hughes mixing model, the Landwehr model (Collins et al., 1997; Motha

27 et al., 2003; Hughes et al., 2009; Collins et al., 2010; Devereux et al., 2010; Gellis and Walling, 2011;
28 Haddadchi et al., 2013). Uncertainties associated to the results of the mixing model are evaluated
29 using mathematical algorithms. In studies dealing with the sediment fingerprinting approach,
30 machine learning algorithms are often applied such as the Bayesian mixing model (Nosrati et al.,
31 2018), Monte-Carlo simulations (Hughes et al., 2009; Lamba et al., 2015; Vale et al., 2016; Pulley and
32 Collins, 2018), classification and regression trees (CART model; Choubin et al., 2018).

33 While the sediment fingerprinting method has largely contributed to the quantification of
34 sources of sediment input for different watersheds around the world, recent discoveries showed that
35 some scientific questions still need to be resolved (e.g. Smith et al., 2015). Some studies have shown
36 that the selection of sources and sediment targets in a catchment may have important implications
37 for the interpretation of the results : highly erodible areas may have a disproportionate effect on
38 tracer concentrations (Wilkinson et al., 2013) and nearby sources may have larger contributions for a
39 given point on a river than distant sources (Haddadchi et al., 2015). It is also important to pre-identify
40 the sources contributing to the sediment flux as an un-sampled source can strongly bias the results
41 (Smith et al., 2015). Thus, the selection of tracers is an important issue in this approach: uncertainties
42 in the prediction of source contributions decrease by increasing the number of trace parameters
43 (Sherriff et al., 2015). Predicted contributions may be different depending on the choice of tracers
44 (Pulley et al., 2015). The conservative behavior of tracers may also introduce bias in interpretations
45 (Sherriff et al., 2015) therefore a careful tracer selection procedure is recommended (Kraushaar et
46 al., 2015). The type and the structure of the mixing model may also affect the results due to different
47 mathematical approaches (see review of Haddadchi et al., 2013; and references therein). Cooper et
48 al. (2014) showed that the estimation of the source contributions varies up to 21% between the
49 different models. Laceby and Olley (2015) suggested that correction factors (particle size or organic
50 matter content) did not significantly improve the results.

51 Existing “black-box” effects related to unknown transport signatures of particles were
52 suggested by Koiter et al. (2013) and are supported by observations published by Fryirs et al. (2013).
53 They suggest that sedimentary transport pathways cannot be assumed to be directly connected
54 between sources and outlets, but include barriers or buffers that disrupt sediment transfer. Recently,
55 Li et al. (2019) show that some element concentrations and their relative contributions to the surface
56 sediments were relevant to sediment transport processes and the related flow paths, because of
57 their association with different types of grains. To address this challenge, the so-called “tributary
58 tracing” or “confluence tracing” approaches were recently developed (e.g. Vale et al., 2016; Nosrati
59 et al., 2018). The latter concept consists in the consideration of tributary upstream sediments as
60 potential sources for downstream sediments, and this approach removes a significant proportion of
61 the impact of potential chemical enrichment on sediments due to particle size variations (Lacey et
62 al., 2017).

63 In the Canche river watershed in Northern France, most natural hazards are related to
64 mudflow and flooding. Mudflow causes significant damages to infrastructure that induce high
65 economic costs. Since 2000, environmental policies are designed to reduce erosion by runoff in the
66 Canche river watershed by implementing hard and soft erosion control measures, such as dams,
67 retention pools, ditches or fascines. However, so far few information is available on the evaluation of
68 the efficiency of these environmental policies.

69 The main goal of this study is to assess the suitability of the confluence-based sediment
70 fingerprinting approach in a relatively homogeneous environmental context and to quantify the
71 contribution of the different tributaries draining the studied agricultural watershed. As this
72 watershed is very sensitive to erosion processes and environmental policies try to reduce the
73 sediment input in the Canche river, this work also proposes an application of the confluence-based
74 sediment fingerprinting approach to evaluate the possible effect of environmental policies on
75 erosion reduction.

76 2. Material & Methods

77 2.1 The Canche river watershed

78 The Canche river watershed (1274 km²; lat.: 50°25'53"N, long.: 2°02'24"E; Fig. 1A) is situated
79 in the European loess belt in Northern France and is characterized by oceanic climate conditions. The
80 mean annual temperature is 11°C and the mean annual rainfall comprises 1000 ± 150 mm. Altitudes
81 range from 0 m at the catchment outlet to 207 m in the upstream areas and catchment slopes are
82 commonly in the range 2-3% (Fig. 1B). The watershed is characterized by a meandriform drainage
83 network dominated by the Canche river (88 km) and seven tributaries. The watershed drains
84 Quaternary loess on the chalky grounds of the Seno-Turonian.

85 The Canche river watershed is dominated by agricultural land use, consisting of 80% arable
86 lands (Fig. 1C). The watershed is affected by mudflows, mainly due to diffuse and concentrate
87 erosion on arable lands that induce an important economic cost for the local communities (Patault,
88 2018). Moreover, surface soils are affected by water erosion leading to a highly variable specific
89 sediment yield at the outlet of the river. The annual sediment export ranged from 29 to 185 kt
90 between 1999 and 2016 according to the local water agency (Agence de l'Eau Artois-Picardie, 2016).

91 The mean annual discharge for the Canche river is estimated to 21 m³ s⁻¹ with contributions
92 from the following main tributaries: Ternoise (7 m³ s⁻¹), Planquette (1.5 m³ s⁻¹), Créquoise (2 m³ s⁻¹),
93 Bras de Bronne (2 m³ s⁻¹), Course (4 m³ s⁻¹), Dordogne (2.5 m³ s⁻¹), and Huîtrepin (2 m³ s⁻¹). The flow
94 discharge was quantified using a low-frequency monitoring station, based on water level estimations,
95 in the Ternoise, Course, and Canche river. Flow discharge for the ungauged catchments $Q_{ungauged}$
96 was calculated assuming similar rainfall and hydrological regimes in the entire watershed. Values
97 were extrapolated from the closest monitoring station by multiplying the value Q_{gauged} with the
98 appropriate fraction related to the ratio between the closest catchment area ($A_{ungauged}$) and the
99 catchment area at the monitoring station A_{gauged} :

$$Q_{ungauged} = Q_{gauged} \times \frac{A_{ungauged}}{A_{gauged}} \quad (1)$$

100

101 with Q representing the discharge in $\text{m}^3 \text{s}^{-1}$ and A as the area of the catchments in km^2 .

102 According to Andréassian et al. (2012), this method provides robust results for ungauged
103 catchments. Cross validation with the high-frequency monitoring station on the Canche river
104 watershed evaluated a 17% associated error (Fig. S1).

105 *2.2 Sediment sampling*

106 Suspended particulate matter (SPM) were collected using sediment traps installed at each
107 tributary outlet and each confluence with the Canche river (Fig. 1D). Sampling campaigns were
108 conducted in winter 2015, winter 2016, spring 2016, summer 2016, and autumn 2016. A total of 65
109 samples was collected. More details on the sampling devices, exact sampling periods, and site
110 positions are available in Figure 2 and Table S1.

111 The samples consist of recently suspended solids transported in the different tributaries.
112 Sediment was sampled using an experimental device adapted from previous studies (described by
113 Tessier (2003) and Kayvantash et al. (2017)). The sediment traps (Fig. 2) consist of 2 l polyethylene
114 bottles, perforated at 5 cm from the top with two opposite holes (diameter 5 cm). The bottle is
115 attached to the river bank with a rope and deposited in the channel. The device is hold in place using
116 either an additional rope or a combination of rope and a wooden beam. The whole device is
117 weighted vertically in the water column using ballast that is adapted to the river flow speed. Traps
118 usually captured between 50 and 100 g of sediments during ~5-7 days water expose. Recent work in
119 the Seine river in France, observed that there is no significant grain size selection depending on the
120 position of the bottle in the river channel (Kayvantash, 2016; Kayvantash et al., 2017).

121 *2.3 Sedimentological and geochemical analysis*

122 All samples were analyzed to obtain particle size distribution and elemental composition.
123 Grain size analyzes were performed using a *Beckman Coulter LS 13320* laser particle sizer. All samples
124 were initially oven-dried at 30°C for 72 h and sieved to 2 mm to remove any coarser debris, such as
125 leafs and roots, that could distort further measurement. Two grams of sediment were mixed with
126 100 ml of ultrapure water and were stirred during 5 min using ultrasonic dispersion to homogenize
127 the sample. Each solution was analyzed in triplicates to validate the measurement.

128 The analysis of the elemental composition was carried out after acid mineralization in a
129 microwave oven. 22 reactors were used for mineralization, 0.250 g of a sample were injected in 18
130 reactors, 2 reactors are used as references with TH2 (reference sediment material) to test the validity
131 of the analysis by comparison with referenced measurements, and 2 blank reactors (without addition
132 of solid material) are used to ensure non-contamination during preparation. For each reactor, 1 ml of
133 nitric acid (HNO₃), 3 ml of hydrochloric acid (HCl), and 0.5 ml of water (H₂O) is added to the sediment.
134 The determination of the major elements in the liquid phase (Al, Ca, Fe, K, Mg, Mn, Na, P, S, Si, Sr, Ti,
135 Zn) was performed using an inductively coupled plasma atomic emission spectrometer (ICP-AES; *ICAP*
136 *7400 Thermo Fischer Scientific*). The determination of the trace elements (As, Ba, Bi, Cd, Ce, Co, Cs,
137 Cr, Cu, La, Li, Mo, Ni, Pb, Rb, Sb, Sc, Se, Sn, Th, Tl, U, V) in the samples was carried out using an
138 inductively coupled plasma mass spectrometer (ICP-MS; *PerkinElmer NexION 300x*).

139 *2.4 Sediment fingerprinting procedure*

140 Several analytical and statistical steps were used, using the model *Sed_Sat-v1.0* (Gorman
141 Sanisaca et al., 2017) to determine which tracers are most significant in defining tributaries and
142 quantifying the relative contributions of tributaries to the suspended sediment samples. The model is
143 written using the statistical software *R* (R Core Team, 2013) and *Microsoft Access*® is used as a user
144 interface.

145 *2.4.1 Test for univariate normal distribution*

146 The following procedure of the Sed_Sat-v1.0 model assumes normality among the analyzed
147 variables. As a first step of the model, all variables were tested for normality, using the Shapiro-Wilk
148 test (Shapiro and Wilk, 1965), to determine if the raw concentration values are normally distributed
149 within each source group. All variables that were not normally distributed were tested again for
150 normality after transformation using the Tukey Ladder of Powers transformations (Table S2; Tukey,
151 1977).

152 2.4.2 Outlier test

153 The average and the standard deviation within each source group for each tracer were
154 determined. If the tracer value for a given source sample exceeded three times the standard
155 deviation of the average value, the sample was considered an outlier and removed from the tracer
156 set (Wainer, 1976; in Gellis et al., 2013).

157 2.4.3 Range test

158 A condition for sediment fingerprinting is that the tracer concentration values in the target
159 dataset must be conservative and do not change during transport (Walling et al., 2002). A range test
160 was used to determine if for any given tracer, the target samples lie within the range of the tracer
161 concentration values in the source dataset. Any tracers that fail to satisfy this condition within the
162 measurement error (10% of each fluvial sample's tracer value) are considered non-conservative and
163 were removed from dataset (Gellis et al., 2013; Gorman Sanisaca et al., 2017).

164 2.4.4 Stepwise Linear Discriminant Function Analysis (DFA)

165 To create the final group of tracers that differentiate the tributaries, a stepwise linear
166 discriminant function analysis (DFA) was performed. The stepwise linear DFA identifies tracers that
167 yield the greatest separation between the tributaries and rejects variables that do not contribute
168 based on the minimization of the Wilk's lambda criterion. The closer the Wilk's lambda statistic is to

169 zero, the more significant a tracer's contribution is to the linear discriminant function. The model
170 selects a combination of tracers that provide optimal separation.

171 2.4.5 Mixing model

172 The remaining set of tracers selected in the stepwise DFA is incorporated into a mixing model
173 to estimate the relative proportion of the sediment source to the target sample. The mixing model
174 was developed and used by Collins et al. (2010). The model uses a set of linear equations for each
175 composite signature by minimizing the sum of squares of the weighted relative errors according to
176 Eq. 2:

$$\sum_{i=1}^n \{ [C_i - (\sum_{s=1}^m P_s S_i)] / C_i \}^2 W_i \quad (2)$$

177

178 Where C_i is the concentration of tracer i in the target sample; P_s is the optimized percentage
179 of contribution source type (s); S_i is the mean concentration of tracer i in source s ; W_i is the
180 weighting factor for tracer i ; n is the number of tracers comprising the optimum composite
181 fingerprint; and m is the number of sediment source types.

182 The model adheres to two constraints that must be satisfied to produce realistic values,
183 which are: each source group proportion is constrain to a positive value between 0 and 1, and is
184 expressed as:

$$0 \leq P_s \leq 1 \quad (3)$$

185 And the sum of all source group contributions has to be equal to 1 and is expressed as:

$$\sum_{s=1}^n P_s = 1 \quad (4)$$

186

187 The tracer discriminatory weighting value, W_i , is used to reflect the tracer discriminatory
188 power, based on the relative discriminatory power of each individual tracer provided by the results
189 of the stepwise DFA. The weighted values ensure that tracers with higher discriminatory power are
190 optimized in the mixing model. The weighting for each tracer that passed the stepwise DFA is
191 calculated as follows:

$$W_i = \frac{P_i}{P_{opt}} \quad (5)$$

192

193 Where P_i is the percentage of correctly classified source samples using tracer i and P_{opt} is the
194 percentage of correctly classified source samples using tracer with the lowest P_i .

195 Tributaries relative contributions were determined for each sample at each confluence with
196 the Canche river. Tributaries percentages are presented for each sampling campaign and were also
197 used to quantify the sediment yield of each tributary.

198 2.4.7 Monte-Carlo simulations and virtual sample mixtures

199 Monte-Carlo simulations were used to evaluate the uncertainties in the confluence-based
200 sediment fingerprinting results produced by the mixing model. The Monte-Carlo simulation randomly
201 removes one sample from each of the eight source type groups and the mixing model is run without
202 these samples. The Monte-Carlo simulation is run 1,000 times on each fluvial sample (Gellis et al.,
203 2015). For each of the 1,000 iterations, the minimum-maximum, and the average sediment source
204 for each tributary are determined. The robustness of the final set of tributaries and tracers is defined
205 using the difference between the final mixing model results, the average, the minimum and
206 maximum source percentage results produced by the Monte-Carlo simulation (Gellis et al., 2013).

207 Virtual sample mixtures are commonly used to assess if mixing model results provide an
208 acceptable range of uncertainty (Haddadchi et al., 2014; Palazón et al., 2015; Pulley and Collins,
209 2018). Thus, we test the robustness of the employed mixing model using tracer values of virtual
210 sample mixtures. These virtual samples consists in hypothetical sediment provenance of equal input
211 from each tributary, and subsequently were mathematically calculated at each confluence. The
212 hypothetical composition of the virtual sample mixtures were then compared to the un-mixed
213 composition calculated by the model. The accuracy of the modelling approach was tested based on
214 the Mean Absolute Error (MAE) at each confluence:

$$MAE = \frac{\sum_{j=1}^m |X_j - Y_j|}{m} \quad (6)$$

215 Where X_j is the hypothetical percentage of each source (j) in mixtures sediments, Y_j is the
216 calculated contribution of each source and m is the number of sources ($m = 8$).

217 2.5 Efficiency of erosion control measures

218 Information on the locations of erosion control measures (runoff retention pools, check
219 dams, fascine, etc.) in the Canche river watershed were provided by the Chamber of Agriculture
220 using the Database *RUISSOL* (Chambre d'Agriculture Nord-Pas-de-Calais, 2013). For each tributary,

221 the number of erosion control measure was extracted. We empirically defined an Erosion Control
222 Index, ECI_i , using the number of erosion control measures installed on each catchment divided by
223 their respective area:

$$ECI_i = \frac{\sum_1^n ECM_i}{A_i} \quad (7)$$

224

225 With ECM_i presenting the number of erosion control measures installed on the catchment i ;
226 and A_i as the area of the catchment i in km^2 . ECI_i was then compared to the annual tributary
227 sediment yield (in kt) calculated using the mixing model and Monte-Carlo simulations.

228 **3. Results**

229 *3.1 Sediment analysis*

230 The particles size analysis highlights the absence of significant differences between the D50
231 (median particle size) of the tributaries ($60.3 \pm 6.7 \mu\text{m}$) in comparison to the sediment sampled at
232 each confluence in the Canche river ($67.9 \pm 10 \mu\text{m}$; Fig. 3). A t-test between the tributaries and the
233 confluences did not show any significant difference between their D50 ($p\text{-value} = 0.107$). Thus for
234 further model analyses, no particle size correction was applied considering that no significant particle
235 size effect affects the direct comparison between tributaries and confluences samples.

236 The geochemical analysis showed evidence of some element concentration heterogeneities
237 for the different sources (Fig. 4). The range of element concentrations is particularly high for some
238 major elements (Ca: $22054.9 - 42314 \mu\text{g g}^{-1}$; S: $1013.4 - 4723.3 \mu\text{g g}^{-1}$) and trace elements (Ce: $29.4 -$
239 $55 \mu\text{g g}^{-1}$; La $16.6 - 30.7 \mu\text{g g}^{-1}$). The element concentrations for the confluences are generally in the
240 range of the values observed for the tributaries. Sometimes the range of the values for confluences is
241 higher than the range for tributaries (Bi, Ca, Cu, Na, and Sr). Even though the Canche river catchment
242 exhibits a homogeneous geology, major and trace elements seem to have a non-negligible potential
243 for discriminating sources and quantify their contribution to the suspended sediment sampled at

244 each confluence. Considering this first approach, robust statistical analyses are needed to explore the
245 entire dataset.

246 *3.2 Final composite fingerprint*

247 The first analysis consisted in the identification of outliers in the source dataset. Results
248 showed no outliers for any tributary. Thus, all tracer parameters were kept for further analysis.
249 Table S3 presents the results of the bracket test and shows that different elements were considered
250 conservative at each sub-basin outlet (spatial sediment sources). Tracers were considered
251 conservative when, for any given tracer, no significant changes during transport between upstream
252 sources and downstream sediment sampling sites occurred. At each confluence, more than twenty
253 tracers were considered conservative and kept for further analysis except for the confluence C2
254 where only nine tracers were considered conservative. Cross validation using bi-plots of tracers of
255 tributary and confluence samples confirmed the conservativeness/non-conservativeness of these
256 tracers (Fig.S2). For the pairs of tracers that are significantly correlated ($R^2 > 0.8$) within the tributary
257 sample dataset, the correlation is maintained when adding the confluence dataset suggesting a high
258 degree of conservatism. For other tracer pairs, the correlation is not maintained when adding the
259 confluence sediment samples, which suggests a non-conservative behaviour. These tracers were
260 correctly identified by the range test and were removed from further analysis.

261 With the remaining set of tracers, the stepwise DFA produced a final composite fingerprint at
262 each confluence that provides sources discrimination (Table 2). The final composite fingerprint
263 includes different chemical tracers that minimizes the Wilk's lambda criterion and that maximizes the
264 source sample discrimination. At each confluence, the proposed final composite fingerprint correctly
265 classified between 53 and 100% of the source samples in their correct affiliation. The classification is
266 better for the confluence C1, C3, and C4, reaching values from 69 to 100%. Chemical tracers selected
267 for the different final composite fingerprint principally include transition metals (44%), metalloids
268 and alkaline earth metals (32%), and other element classes (24%; alkali metals, nonmetals,

269 lanthanides and actinides). Selected tracers are appropriate, considering the geochemical
270 background level of the Canche watershed and the point or non-point discharges mainly induced by
271 agricultural activity.

272 *3.3 Monte-Carlo simulations*

273 The range of Monte-Carlo simulations results show difference of $\pm 10\%$ in comparison with
274 the average resulting from the mixing model (Fig.S3). The relative contributions calculated by the
275 mixing model at each confluence are considered robust, despite a large spread of the Monte-Carlo
276 results between minimum and maximum values can be observed for some confluences (C2 - C5).
277 Nevertheless, the increase of sources, after confluence C5, tends to decrease the uncertainties in the
278 Monte-Carlo simulations.

279 Modelling results using virtual mixtures at each confluence confirm that all sources are well
280 recognized by the mixing model (Fig.5). The MAE values are relatively low and are thus considered
281 acceptable, ranging from 0.93 to 6.36%, with a slight variability within each confluence (min = 0.27
282 and max = 7.57%). The results are considered robust, even with a high number of sources at the last
283 confluence (m = 8 and MAE = 2.1%). This test supports the hypothesis that the applied methodology
284 is reliable.

285 *3.4 Annual tributaries contributions*

286 Annual tributaries relative contributions could be calculated using the four campaigns
287 performed during the year 2016 (Fig. 6). The results show in general a high and persistent relative
288 contribution of the Planquette and the Créquoise along the main channel. For example, the relative
289 contribution of the Planquette at point C3 is 19% and 21% at point C7. The contributions of the
290 upstream part of the Canche river and the Ternoise are particularly high in the upstream areas (33
291 and 49% at point C2) but tend to decrease as we approach the outlet of the catchment (12 and 3% at
292 point C7). The relative contribution of the Course seems important in the downstream area except
293 for the point C6 that may have encountered a mis-classification of the source samples (C5: 24% -; C6:

294 3%; C7: 15%). The relative contributions of the downstream tributaries (Dordogne and Huîtrepin) are
295 generally moderate as their outlet is closer to the sampling point. These average results over four
296 sampling campaigns corresponding to the hydrologic year 2016 seem consistent if we consider the
297 relative hydrological contributions of each tributary to the Canche main stream and the length of the
298 main channel. Spatial variations show that along the Canche river catchment, the sedimentary
299 signatures of the upstream tributaries tend to decrease as we approach the downstream indicating a
300 possible effect of storage and/or dilution of the sediment flux.

301 *3.5 Tributaries sediment yield*

302 Considering the information provided by the Artois-Picardie Water Agency, the annual
303 sediment yield of the Canche river catchment ranges from 29 to 185 kt yr⁻¹ since 1999. The relative
304 contributions were previously evaluated at point C7 as follows: Canche 12%, Ternoise 3%, Planquette
305 22%, Créquoise 20%, Bras de Bronne 7%, Course 15%, Dordogne 6%, and Huîtrepin 15%. Based on
306 the lower and upper boundaries of the annual sediment yield, the range of the sediment yield and
307 specific sediment yield from tributaries to the main stream were calculated (Table S3). The highest
308 sediment yields were calculated for the Créquoise and the Planquette, 5.8 – 37 kt yr⁻¹ and
309 respectively 6.38 – 40.7 kt yr⁻¹. The lowest sediment yields were estimated for the Ternoise (0.87 –
310 5.55 kt yr⁻¹), the Bras de Bronne (2.03 – 12.95 kt yr⁻¹), and the Dordogne (1.74 – 11.1 kt yr⁻¹).

311 *3.6 Impact of erosion control measures*

312 Considering that catchment stakeholders implemented 1590 erosion control measures in the
313 Canche river watershed since 2000, this study proposes to evaluate their efficiency using the defined
314 erosion control index (ECI_i) and the sediment yield of each tributary previously calculated. Here, we
315 solely implement the total number of the measures installed, as considered parameter in the ECI_i .
316 We precise that there exist several types of erosion control measures in the field (fascines, grass
317 strips, hedges, ponds, dams, nozzles, ditches). Nevertheless, the ratio between the different types of
318 measures is similar whatever the treated catchment. Our results show a positive impact of the

319 installation of erosion control measures. Catchments characterized by flow discharge around $1 \text{ m}^3 \text{ s}^{-1}$
320 with the highest ECI_i (Dordogne, Bras de Bronne, Huîtrepin) exhibit low values of sediment yield
321 (Fig. 7). For catchments with similar fluxes and for which few erosion control measures were installed
322 so far (Créquoise, Planquette, Course), high values of sediment yield are observed. The relation
323 between sediment yield and ECI_i decreases as the number of erosion control measures increases on
324 a catchment. These results are consistent with the environmental policies of the last decades and
325 confirm their benefits. The upstream and middle catchments all present a low ECI_i (~ 1). The
326 upstream Canche and Ternoise catchments characterized by large areas show a high flow discharge.
327 Surprisingly the suspended matter flux is much lower than for the other catchments. It is suggested
328 that large catchment areas with high flow discharge are also those where the proportion of erosion-
329 sensitive surfaces is lower than for small catchments. We also assume a preferential deposit of their
330 sediment contribution in the upstream part of their respective river channel.

331 *3.7 Seasonal variability of tributaries contributions*

332 The seasonal contribution of each tributary at each confluence was estimated for the five
333 sampling campaigns (Fig. 6). An important seasonal variability can be observed along with major
334 fluctuations in relative source contributions. In general, we can observe an important relative
335 contribution of the upstream tributaries (Canche upstream, Ternoise, Planquette, and Créquoise).
336 The downstream tributaries (Bras de Bronne, Course, Dordogne, and Huîtrepin) exhibit lower
337 contributions to the sediment yield except for the Bras de Bronne in winter 2015 and summer 2016,
338 and for the Course in winter and spring 2016. For the upstream tributaries, the influence of the
339 Planquette is more effective in dry seasons: summer and spring 2016, the influence of the Créquoise
340 is more effective during wet seasons: winter and autumn 2016. The relative contribution of the
341 Canche is more pronounced during winter and spring 2016 whereas for the Ternoise, the relative
342 contribution is greater in summer and autumn 2016. An effect of storage and/or dilution can be
343 easily observed along the main channel of the Canche river. The relative contributions of the
344 upstream catchments generally decrease when approaching of the downstream sections. Moreover,

345 relative contributions of some downstream tributaries, such as the Dordogne or the Bras de Bronne,
346 generally decrease near the sampling point (outlet of the respective tributary).

347 **4. Discussion**

348 *4.1 Meaningful implications for erosion control strategies*

349 The quantification of the tributaries relative contributions using a confluence-based
350 sediment fingerprinting approach was quite conclusive, even in this relatively homogeneous
351 lithological context comprising silty soils which as highly sensitive to erosion processes. The sampling
352 strategy deployed was original and spatially representative of the catchment, following the need for
353 robust sediment fingerprinting approaches as stated by several authors (Smith et al., 2015; Laceby et
354 al., 2017). This approach was based on a relatively simple but effective field methodology on selected
355 strategic sampling points, collecting suspended particulate matter with sediment traps in the Canche
356 watershed at each tributary and each confluence. Time-integrated sediment traps have appeared as
357 very suitable experimental devices to sample a large amount of suspended sediment matter during a
358 restricted sampling period and to study sediment fluxes fluctuations. As stated e.g. by Phillips et al.
359 (2000), Russell et al. (2000), or recent sediment fingerprinting studies on suspended sediment by e.g.
360 Huisman et al. (2013) and Lamba et al. (2015), the use of comparable time-integrated sampling
361 devices is much more representative for this kind of study than point sampling. According to Walling
362 and Webb (1987), sediment transport is highly episodic (90% of annual load is transported within
363 only 10% of the time).

364 The confluence-based approach developed in this study was also particularly effective. As
365 emphasized by Vale et al. (2016), the short distance between upstream and downstream sediment
366 samples limits the effect that non-conservative behavior has on geochemical signature uncertainties.
367 The use of geochemical tracers was relevant in the Canche river watershed, even regarding the
368 homogeneous lithological context, because of significant element composition differences between
369 the tributaries. Differences are assumed to be mainly driven by lithological background level and the

370 point or non-point discharge induced by agricultural activities. The results of the simulations showed
371 that tributaries located in the central part of the Canche river watershed (Planquette, Créquoise)
372 were the most contributing to the sediment yield. They also highlight contrasted responses from one
373 season to another, certainly in relation to rains entailing erosive event, which concern in a short
374 time, a localized area.

375 This work provided conclusions to estimate the spatial evolution of erosive dynamics over a
376 considerably wide area, particularly in relation to the development plans of erosion control facilities.
377 These methodologies can successfully locate the most contributing areas in term of erosion. The
378 results of the study also showed that the environmental policies of the last decades in Northern
379 France seem effective, confirming the recent observations made by Frankl et al. (2017). For
380 catchments with similar areas and fluxes, those with the less erosion control measures installed,
381 exhibit the highest relative contributions to the sediment yield. To our knowledge, this study is the
382 first one comparing results from a confluence-based sediment fingerprinting approach to the land
383 management policies on a watershed. The results are significant, particularly in the given
384 homogeneous context, which enhances the novelty of the approach and thus should be tested for
385 other environmental contexts taking into account the specificities of the studied catchment.

386 *4.2 Limitations and uncertainties*

387 The tributaries contributions quantified in this study using the confluence-based sediment
388 fingerprinting approach must be interpreted in the context of some limitations and uncertainties.
389 The target river sediment for source apportionment was collected from a single downstream location
390 for each tributary. The estimated catchment proportions at each confluence therefore strongly relate
391 to the respective sampling site. Koiter et al. (2013) pointed out that sources estimates are scale-
392 dependent and can differ for sampling locations along a channel network. This limitation, the so-
393 called “black-box”, remains one of the largest limitations of the sediment fingerprinting approach.

394 Sediment sampling also needs to be temporally representative. Our approach addresses this
395 question with a seasonal sampling, although our tributaries estimations are representative of five
396 weeks over two years. It is likely that multiple major flood event could have transported a significant
397 proportion of the annual sediment load and may have not been sampled here. Automatic sediment
398 samplers could be deployed on each key location to increase the temporal representability with the
399 big disadvantage that much more sampling logistics would be needed. Considering these limitations,
400 two approaches need to be explored. First, we may suggest the use of other sediment traps, which
401 offers a larger sediment storage capacity and that can be dropped at key locations during a few
402 months. Secondly, as suggested by Guzmán et al. (2013), we may suggest finding other tracers
403 requiring inexpensive and rapid analysis approach to process quickly a large number of samples. This
404 seems feasible using the spectrophotometric or magnetic tracers (Krein et al., 2003; Legout et al.,
405 2013; Patault, 2018). They allow rapid, non-destructive and quantitative measurements of soil and
406 sediment property.

407 Although tracer properties were tested for transformation using the range test, this does not
408 confirm the complete absence of tracer property transformation during sediment delivery. As shown
409 by Sherriff et al. (2015), the non-conservative behavior of a single tracer property included in a mass
410 balance mixing model can affect the predicted source contributions. According to Zhang and Liu
411 (2016), a more stringent statistical analysis than only the bracket test comprised in the *Sed_Sat-v1.0*
412 model, could be proposed to confirm the absence of non-conservative tracers using mixing polygon
413 test. Moreover, Kraushaar et al. (2015) suggested an expanded procedure including water sample
414 analyses to identify tracers that may be susceptible to dissolution during transport. Using the
415 sediment traps deployed in this study, the experiment could be easily done. Further research in this
416 way is strongly recommended.

417 Particle size effect on element concentration remains one of the biggest uncertainties in
418 sediment fingerprinting approach. Differences between sources and downstream sediments may

419 arise from selective transport (Koiter et al., 2015). Our confluence-based approach, as shown in the
420 work of Vale et al. (2016) and Nosrati et al. (2018), decreases the effect that particle size can exert on
421 predicted source contributions. Our analysis proves that the median particle size (D50) was
422 practically the same for all tributary and confluence samples, and thus no correction factor were
423 applied. For future research, the confluence-based approach should be largely explored.

424 Virtual sample mixtures considering hypothetical tributary provenance (e.g. equal inputs)
425 confirmed the robustness of the applied methodology. Uncertainties were relatively low, showing
426 only slight evidence of variability within each confluence. However, virtual sample mixtures still
427 remain hypothetical, experiments on artificial sample mixtures of known sediment proportions as
428 suggested by Pulley and Collins (2018) would help further refine the modelling results. Also, as
429 suggested by Pulley et al. (2015), tracer selection must maximize contrasts in tracer concentrations
430 between all sources. In the case of the Canche river watershed, which shows a very homogeneous
431 geology; existing but slight differences between the source tracers concentrations were observed.
432 Considering this, we suggest increasing the number and the type of tracers by addition of more
433 discriminating parameters related to the typology of the organic matter.

434 **5. Conclusions**

435 The study successfully shows that a confluence-based sediment fingerprinting approach
436 using time-integrated samplers (sediment traps) and physico-chemical analyses on suspended
437 sediment matter, allows discriminating the relative sediment yield contribution of the different
438 tributaries that compose a given catchment, even in a homogeneous lithological context. Best tracers
439 able to discriminate the tributaries (transition metals, metalloids, and alkaline earth metals) were
440 identified using statistical analyses and were incorporated into a mass balance mixing model
441 (*Sed_Sat-v1.0 model*). Discriminating tracers were assumed to be mainly driven by the lithological
442 background level and the point/non-point discharge induced by agricultural activities. Annual
443 tributary contributions were evaluated and range from 3 to 22% at the outlet of the main stream.

444 Validation using virtual sample mixtures allow considering that the methodology presented is robust.
445 Considering information given by the Artois-Picardie Water Agency, the annual tributary sediment
446 delivery actually ranges from 0.87 to 40.7 kt yr⁻¹. The Planquette and the Créquoise were considered
447 as the most erosive tributaries of the Canche watershed. Tributaries with the highest number of
448 installed erosion control measures on the territory exhibit the lowest values of sediment export
449 confirming the generally positive impact of recent land management policies in Northern France. This
450 novel approach allows to evaluate the relevance of environmental strategies to reduce water erosion
451 in the studied watershed, and easily provides helpful information on decision support for future land
452 management.

453 **Acknowledgements**

454 This work was financially supported by the Mines-Telecom Institute of Lille-Douai, with
455 additional funding provided by the Artois-Picardie Water Agency (QUASPER project). We would also
456 like to acknowledge technical support from the SYMCEA and the regional Chamber of Agriculture
457 Nord-Pas-de-Calais, France. The authors are grateful to L. Alleman and B. Malet for the *ICP-MS/AES*
458 analyses (IMT Lille-Douai – SAGE department). The authors thanks A. Gellis and L. Gorman Sanisaca
459 (USGS) who provided the *Sed_Sat-v1.0* model and for their helpful discussions. The authors also
460 thanks the four anonymous reviewers who provided constructive suggestions to improve the
461 manuscript.

462 **References**

- 463 Agence de l'eau Artois-Picardie. (2016). *Schéma Directeur d'Aménagement et de Gestion des Eaux du*
464 *Bassin Artois-Picardie*. Retrieved from <http://www.eau-artois-picardie.fr/sdage>
- 465 Carter, J., Owens, P., Walling, D., & Leeks, G. (2003). Fingerprinting suspended sediment sources in a
466 large urban river system. *The Science of The Total Environment*, 314–316(03), 513–534.
467 [https://doi.org/10.1016/S0048-9697\(03\)00071-8](https://doi.org/10.1016/S0048-9697(03)00071-8)
- 468 Chambre d'agriculture Nord-Pas-de-Calais. (2013). RUISSOL: Outil de gestion des données liées au
469 suivi des ouvrages de lutte contre l'érosion des sols agricoles.
470 <https://www.ruissol.pro/CGI/DLL.dll?APP=3&MODULE=Ruissol>
- 471 Choubin, B., Darabi, H., Rahmati, O., Sajedi-Hosseini, Kløve, B. (2018). River suspended sediment
472 modelling using the CART model: A comparative study of machine learning techniques. *Science*

- 473 *of the Total Environment*, 615, 272-281. <https://doi.org/10.1016/j.scitotenv.2017.09.293>
- 474 Collins, A. L., Walling, D. E., & Leeks, G. J. L. (1997). Use of the geochemical record preserved in
475 floodplain deposits to reconstruct recent changes in river basin sediment sources.
476 *Geomorphology*, 19, 151–167. [https://doi.org/10.1016/S0169-555X\(96\)00044-X](https://doi.org/10.1016/S0169-555X(96)00044-X)
- 477 Collins, A. L., Walling, D. E., Sickingabula, H. M., Leeks, G. J. L. (2001). Suspended sediment source
478 fingerprinting in a small tropical catchment and some management implications. *Applied*
479 *Geography*, 21(4), 387–412. [https://doi.org/10.1016/S0143-6228\(01\)00013-3](https://doi.org/10.1016/S0143-6228(01)00013-3)
- 480 Collins, A. L., & Walling, D. E. (2002). Selecting fingerprint properties for discriminating potential
481 suspended sediment sources in river basins. *Journal of Hydrology*, 261, 218–244.
482 [https://doi.org/10.1016/S0022-1694\(02\)00011-2](https://doi.org/10.1016/S0022-1694(02)00011-2)
- 483 Collins, A. L., Walling, D. E., Webb, L., King, P. (2010). Apportioning catchment scale sediment sources
484 using a modified composite fingerprinting technique incorporating property weightings and
485 prior information. *Geoderma*, 155(3–4), 249–261.
486 <https://doi.org/10.1016/j.geoderma.2009.12.008>
- 487 Collins, A. L., Zhang, Y., McChesney, D., Walling, D. E., Haley, S. M., Smith, P. (2012). Sediment source
488 tracing in a lowland agricultural catchment in southern England using a modified procedure
489 combining statistical analysis and numerical modelling. *Science of The Total Environment*, 414,
490 301–317. <https://doi.org/10.1016/j.scitotenv.2011.10.062>
- 491 Cooper, R. J., Krueger, T., Hiscock, K. M., & Rawlins, B. G. (2014). Sensitivity of fluvial sediment source
492 apportionment to mixing model assumptions: A Bayesian model comparison. *Water Resources*
493 *Research*, 50(11), 9031–9047. <https://doi.org/doi:10.1002/2014WR016194>
- 494 Du, P., & Walling, D. E. (2016). Fingerprinting surficial sediment sources: Exploring some potential
495 problems associated with the spatial variability of source material properties. *Journal of*
496 *Environmental Management*, 1–12. <https://doi.org/10.1016/j.jenvman.2016.05.066>
- 497 Evrard, O., Navratil, O., Ayrault, S., Ahmadi, M., Némery, J., Legout, C., Esteves, M. (2011). Combining
498 suspended sediment monitoring and fingerprinting to determine the spatial origin of fine
499 sediment in a mountainous river catchment. *Earth Surface Processes and Landforms*, 36(8),
500 1072–1089. <https://doi.org/10.1002/esp.2133>
- 501 Evrard, O., Poulénard, J., Némery, J., Ayrault, S., Gratiot, N., Duvert, C., Esteves, M. (2013). Tracing
502 sediment sources in a tropical highland catchment of central Mexico by using conventional and
503 alternative fingerprinting methods. *Hydrological Processes*, 27(6), 911–922.
504 <https://doi.org/10.1002/hyp.9421>
- 505 Frankl, A., Prêtre, V., Nyssen, J., Salvador, P-G. (2017). The success of recent land management
506 efforts to reduce soil erosion in northern France. *Geomorphology*, 303, 84–93.
507 <https://doi.org/10.1016/j.geomorph.2017.11.018>
- 508 Fryirs, K., & Gore, D. (2013). Sediment tracing in the upper Hunter catchment using elemental and
509 mineralogical compositions: Implications for catchment-scale suspended sediment
510 (dis)connectivity and management. *Geomorphology*, 193, 112–121.
511 <https://doi.org/10.1016/j.geomorph.2013.04.010>
- 512 Gellis, A. C., & Walling, D. E. (2011). Sediment Source Fingerprinting (Tracing) and Sediment Budgets
513 as Tools in Targeting River and Watershed Restoration Programs. *Geophysical Monograph*
514 *Series*, 194(JANUARY), 263–291. <https://doi.org/10.1029/2010GM000960>

- 515 Gellis, A. C., & Noe, G. B. (2013). Sediment source analysis in the Linganore Creek watershed,
516 Maryland, USA, using the sediment fingerprinting approach: 2008 to 2010. *Journal of Soils and*
517 *Sediments*, 13 (10), 1735-1753. <https://doi.org/10.1007/s11368-013-0771-6>
- 518 Gellis, A. C., Noe, G. B., Clune, J. W., Myers, M. K., Hupp, C. R., Schenk, E. R., Schwarz, G. E. (2015).
519 Sources of the grained sediment in the Linganore Creek watershed, Frederick and Carroll
520 Counties, Maryland, 2008-10: U.S. Geological Survey Scientific Investigations Report 2014-5147,
521 56p., <http://dx.doi.org/10.31313/sir20145147>.
- 522 Gorman Sanisaca, L. E., Gellis, A. C., & Lorenz, D. L. (2017). Determining the Sources of Fine-Grained
523 Sediment Using the Sediment Source Assessment Tool (Sed _ SAT): U.S. Geological Survey
524 Open File Report 2017-1062, 104 p., <https://doi.org/10.3133/ofr20171062>.
- 525 Guzmán, G., Quinton, J. N., Nearing, M. A., Mabit, L., Gómez, J. A. (2013). Sediment tracers in water
526 erosion studies: current approaches and challenges. *Journal of Soils and Sediments*, 13(4), 816–
527 833. <https://doi.org/10.1007/s11368-013-0659-5>
- 528 Haddadchi, A., Ryder, D. S., Evrard, O., Olley, J. (2013). Sediment fingerprinting in fluvial systems:
529 review of tracers, sediment sources and mixing models. *International Journal of Sediment*
530 *Research*, 28(4), 560–578. [https://doi.org/10.1016/S1001-6279\(14\)60013-5](https://doi.org/10.1016/S1001-6279(14)60013-5)
- 531 Haddadchi, A., Olley, J. & Laceby, P. (2014). Accuracy of mixing models in predicting sediment source
532 contributions. *Science of the Total Environment*, 497-498, 139-152.
533 <https://dx.doi.org/10.1016/j.scitotenv.2014.07.105>
- 534 Haddadchi, A., Olley, J., & Pietsch, T. (2015). Quantifying sources of suspended sediment in three size
535 fractions. *Journal of Soils and Sediments*, 15(10), 2086-2100. <https://doi.org/10.1007/s11368-015-1196-1>
- 537 Hughes, A. O., Olley, J. M., Croke, J. C., McKergow, L. A. (2009). Sediment sources changes over the
538 last 250 years in a dry-tropical catchment, central Queensland, Australia. *Geomorphology*,
539 104(3-4), 262–275. <https://doi.org/10.1016/j.geomorph.2008.09.003>
- 540 Huisman, N. L. H., Karthikeyan, K. G., Lamba, J., Thompson, A. M., Peaslee, G. (2013). Quantification
541 of seasonal sediment and phosphorus transport dynamics in an agricultural watershed using
542 radiometric fingerprinting techniques. *Journal of Soils and Sediments*, 13(10), 1724-1734.
543 <https://doi.org/10.1007/s11368-013-0796-0>
- 544 Kayvantash, D. (2016). *Caractérisation des particules ferrugineuses dans la Seine avec le magnétisme*
545 *environnemental*. Thèse de doctorat. Université de recherche Paris Sciences et Lettres, France.
546 268p.
- 547 Kayvantash, D., Cojan, I., Kissel, C., Franke, C. (2017). Magnetic fingerprint of the sediment load in a
548 meander bend section of the Seine River (France). *Geomorphology*, 286, 14–26.
549 <https://doi.org/10.1016/j.geomorph.2017.02.020>
- 550 Koiter, A. J., Owens, P. N., Petticrew, E. L., Lobb, D. A. (2013). The behavioural characteristics of
551 sediment properties and their implications for sediment fingerprinting as an approach for
552 identifying sediment sources in river basins. *Earth-Science Reviews*, 125, 24–42.
553 <https://doi.org/10.1016/j.earscirev.2013.05.009>
- 554 Koiter, A. J., Owens, P. N., Petticrew, E. L., Lobb, D. A. (2015). The role of gravel channel beds on the
555 particle size and organic matter selectivity of transported fine-grained sediment: implications
556 for sediment fingerprinting and biogeochemical flux research. *Journal of Soils and Sediments*,
557 15(10), 2174–2188. <https://doi.org/10.1007/s11368-015-1203-6>

- 558 Kraushaar, S., Schumann, T., Ollesch, G., Schubert, M., Vogel, H.-J., Siebert, C. (2015). Sediment
559 fingerprinting in northern Jordan: element-specific correction factors in a carbonatic setting.
560 *Journal of Soils and Sediments*, 15(10), 2155–2173. <https://doi.org/10.1007/s11368-015-1179-2>
- 561 Krein, A., Petticrew, E., & Udelhoven, T. (2003). The use of fine sediment fractal dimensions and
562 colour to determine sediment sources in a small watershed. *Catena*, 53(2), 165–179.
563 [https://doi.org/10.1016/S0341-8162\(03\)00021-3](https://doi.org/10.1016/S0341-8162(03)00021-3)
- 564 Lacey, J. P., Evrard, O., Smith, H. G., Blake, W. H., Olley, J. M., Minella, J. P. G., Owens, P. N. (2017).
565 The challenges and opportunities of addressing particle size effects in sediment source
566 fingerprinting: A review. *Earth-Science Reviews*, 169, 85–103.
567 <https://doi.org/10.1016/j.earscirev.2017.04.009>
- 568 Lacey, J. P., & Olley, J. (2015). An examination of geochemical modelling approaches to tracing
569 sediment sources incorporating distribution mixing and elemental correlations. *Hydrological*
570 *Processes*, 29(6), 1669–1685. <https://doi.org/10.1002/hyp.10287>
- 571 Lamba, J., Karthikeyan, K. G., & Thompson, A. M. (2015). Apportionment of suspended sediment
572 sources in an agricultural watershed using sediment fingerprinting. *Geoderma*, 239–240, 25–33.
573 <https://doi.org/10.1016/j.geoderma.2014.09.024>
- 574 Le Gall, M., Evrard, O., Foucher, A., Lacey, J. P., Salvador-Blanes, S., Thil, F., Ayrault, S. (2016).
575 Quantifying sediment sources in a lowland agricultural catchment pond using ¹³⁷Cs activities
576 and radiogenic ⁸⁷Sr/⁸⁶Sr ratios. *Science of the Total Environment*, 566–567, 968–980.
577 <https://doi.org/10.1016/j.scitotenv.2016.05.093>
- 578 Legout, C., Poulenard, J., Nemery, J., Navratil, O., Grangeon, T., Evrard, O., Esteves, M. (2013).
579 Quantifying suspended sediment sources during runoff events in headwater catchments using
580 spectroradiometry. *Journal of Soils and Sediments*, 13(8), 1478–1492.
581 <https://doi.org/10.1007/s11368-013-0728-9>
- 582 Li, T., Sun, G., Yang, C., Liang, K., Ma, S., Huang, L., Luo, W. (2019). Source apportionment and source-
583 to-sink transport of major and trace elements in coastal sediments: Combining positive matrix
584 factorization and sediment trend analysis. *Science of the Total Environment*, 651, 344–356.
585 <https://doi.org/10.1016/j.scitotenv.2018.09.198>
- 586 Martínez-Carreras, N., Udelhoven, T., Krein, A., Gallart, F., Iffly, J. F., Ziebel, J., Walling, D. E. (2010).
587 The use of sediment colour measured by diffuse reflectance spectrometry to determine
588 sediment sources: Application to the Attert River catchment (Luxembourg). *Journal of*
589 *Hydrology*, 382(1–4), 49–63. <https://doi.org/10.1016/j.jhydrol.2009.12.017>
- 590 Motha, J. A., Wallbrink, P. J., Hairsine, P. B., Grayson, R. B. (2003). Determining the sources of
591 suspended sediment in a forested catchment in southeastern Australia. *Water Resources*
592 *Research*, 39(3), 1056. <https://doi.org/10.1029/2001wr000794>
- 593 Motha, J. A., Wallbrink, P. J., Hairsine, P. B., Grayson, R. B. (2004). Unsealed roads as suspended
594 sediment sources in an agricultural catchment in south-eastern Australia. *Journal of Hydrology*,
595 286(1–4), 1–18. <https://doi.org/10.1016/j.jhydrol.2003.07.006>
- 596 Nosrati, K., Collins, A. L., & Madankan, M. (2018). Fingerprinting sub-basin spatial sediment sources
597 using different multivariate statistical techniques and the Modified MixSIR model. *Catena*, 164,
598 32–43. <https://doi.org/10.1016/j.catena.2018.01.003>
- 599 Palazón, L., Latorre, B., Gaspar, L., Blake, W. H., Smith, H. G., Navas, A. (2015). Comparing catchment
600 sediment fingerprinting procedures using an auto-evaluation approach with virtual sample

- 601 mixtures. *Science of The Total Environment*, 532, 456–466.
602 <https://doi.org/10.1016/j.scitotenv.2015.05.003>
- 603 Patault, E. (2018). *Analyse multi-échelle des processus d'érosion hydrique et de transferts*
604 *sédimentaires en territoire agricole: exemple du bassin versant de la Canche*. Thèse de doctorat.
605 IMT Lille Douai, France. 300p.
- 606 Phillips, J. M., Russell, M. A., & Walling, D. E. (2000). Time-integrated sampling of fluvial suspended
607 sediment: a simple methodology for small catchments. *Hydrological Processes*, 14(14), 2589-
608 2602. [https://doi.org/10.1002/1099-1085\(20001015\)14:14<2589::AID-HYP94>3.0.CO;2-D](https://doi.org/10.1002/1099-1085(20001015)14:14<2589::AID-HYP94>3.0.CO;2-D)
- 609 Poulenard, J., Perrette, Y., Fanget, B., Quetin, P., Trevisan, D., Dorioz, J. M. (2009). Infrared
610 spectroscopy tracing of sediment sources in a small rural watershed (French Alps). *Science of*
611 *the Total Environment*, 407(8), 2808–2819. <https://doi.org/10.1016/j.scitotenv.2008.12.049>
- 612 Pulley, S., Foster, I., & Antunes, P. (2015). The application of sediment fingerprinting to floodplain
613 and lake sediment cores: assumptions and uncertainties evaluated through case studies in the
614 Nene Basin, UK. *Journal of Soils and Sediments*, 15(10), 2132-2154.
615 <https://doi.org/10.1007/s11368-015-1136-0>
- 616 Pulley, S. & Collins, A. L. (2018). Tracing catchment fine sediment sources using the new SIFT
617 (Sediment Fingerprinting Tool) open source software. *Science of the Total Environment*, 635,
618 838–858. <https://doi.org/10.1016/j.scitotenv.2018.04.126>
- 619 R Core Team (2013). R: A language and environment for statistical computing. R Foundation for
620 statistical computing, Vienna, Austria. URL: <http://www.R-project.org/>
- 621 Russell, M. A., & Walling, D. E. (2000). Appraisal of a simple sampling device for collecting time-
622 integrated fluvial suspended sediment samples. *The Role of Erosion and Sediment Transport in*
623 *Nutrient and Contaminant Transfer (Proceedings of a symposium held at Waterloo, Canada,*
624 *July 2000)*. IAHS Publ. no. 263.
- 625 Russell, M. A., Walling, D. E., & Hodgkinson, R. . (2001). Suspended sediment sources in two small
626 lowland agricultural catchments in the UK. *Journal of Hydrology*, 252(1–4), 1–24.
627 [https://doi.org/10.1016/S0022-1694\(01\)00388-2](https://doi.org/10.1016/S0022-1694(01)00388-2)
- 628 Shapiro, S. S., & Wilk, M. B. (1965). An Analysis of Variance Test for Normality (Complete Samples),
629 52(3), 591–611. Retrieved from <http://www.jstor.org/stable/2333709>
- 630 Sherriff, S. C., Franks, S. W., Rowan, J. S., Fenton, O., Ó'hUallacháin, D. (2015). Uncertainty-based
631 assessment of tracer selection, tracer non-conservativeness and multiple solutions in sediment
632 fingerprinting using synthetic and field data. *Journal of Soils and Sediments*, 15(10), 2101-2116.
633 <https://doi.org/10.1007/s11368-015-1123-5>
- 634 Smith, H. G., Evrard, O., Blake, W. H., Owens, P. N. (2015). Preface—Addressing challenges to
635 advance sediment fingerprinting research. *Journal of Soils and Sediments*, 15(10), 2033-2037.
636 <https://doi.org/10.1007/s11368-015-1231-2>
- 637 Tessier, L. (2003). *Transport et caractérisation des matières en suspension dans le bassin versant de la*
638 *Seine : identification de signatures naturelles et anthropiques*. Thèse de doctorat. Ecole des
639 Ponts ParisTech.
- 640 Theuring, P., Collins, A. L., & Rode, M. (2015). Source identification of fine-grained suspended
641 sediment in the Kharaa River basin, northern Mongolia. *Science of The Total Environment*, 526,
642 77–87. <https://doi.org/10.1016/j.scitotenv.2015.03.134>

- 643 Vale, S. S., Fuller, I. C., Procter, J. N., Basher, L. R., Smith, I. E. (2016). Application of a confluence-
644 based sediment-fingerprinting approach to a dynamic sedimentary catchment, New Zealand.
645 *Hydrological Processes*, 30(5), 812–829. <https://doi.org/10.1002/hyp.10611>
- 646 Vale, S. S., Fuller, I. C., Procter, J. N., Basher, L. R., Smith, I. E. (2016). Characterization and
647 quantification of suspended sediment sources to the Manawatu River, New Zealand. *Science of*
648 *the Total Environment*, 543, 171-186. <https://doi.org/10.1016/j.scitotenv.2015.11.003>
- 649 Venables, W. N. & Ripley, B. D. (2002). *Modern Applied Statistics With S. Technometrics*.
650 <https://doi.org/10.1198/tech.2003.s33>
- 651 Walling, D. E., Russell, M. A., Hodgkinson, R. A., Zhang, Y. (2002). Establishing sediment budgets for
652 two small lowland agricultural catchments in the UK. *Catena*, 47(4), 323–353.
653 [https://doi.org/10.1016/S0341-8162\(01\)00187-4](https://doi.org/10.1016/S0341-8162(01)00187-4)
- 654 Walling, D. E. & Webb, B. W. (1987). Suspended load in gravel bed-rivers: UK experience, in Thorne,
655 C. R., Bathurst, J. C. and Hey, R. D. (Eds). *Sediment transportation in Gravel-bed river*. Wiley,
656 Chichester, pp. 691-723.
- 657 Walling, D. E. & Woodward, J. C. (1992). Use of radiometric fingerprints to derive information on
658 suspended sediment sources. Erosion and Sediment Transport Monitoring Programmes in River
659 Basins. (Proceedings Oslo Symposium). In *Erosion and sediment transport Programmes in River*
660 *Basins* (Vol. 210, pp. 64–153).
- 661 Walling, D. E., Woodward, J. C., & Nicholas, A. P. (1993). A multi-parameter approach to fingerprint
662 suspended-sediment sources. In *Tracers in Hydrology (Proceeding of the Yokohama Symposium,*
663 *July 1993)*. IAHS Publ. no, 215.
- 664 Weihs, C., Ligges, U., Luebke, K., Raabe, N. (2005). klaR: analyzing German business cycles. *Data*
665 *Analysis and Decision Support*, 335–343. https://doi.org/10.1007/3-540-28397-8_36
- 666 Wilkinson, S. N., Hancock, G. J., Bartley, R., Hawdon, A. A., Keen, R. J. (2013). Using sediment tracing
667 to assess processes and spatial patterns of erosion in grazed rangelands, Burdekin River basin,
668 Australia. *Agriculture, Ecosystems and Environment*, 180, 90–102.
669 <https://doi.org/10.1016/j.agee.2012.02.002>
- 670 Zhang, X. C., & Liu, B. L. (2016). Using multiple composite fingerprints to quantify fine sediment
671 source contributions: a new direction. *Geoderma*, 268, 108-118.
672 <https://doi.org/10.1016/j.geoderma.2016.01.031>

Figures

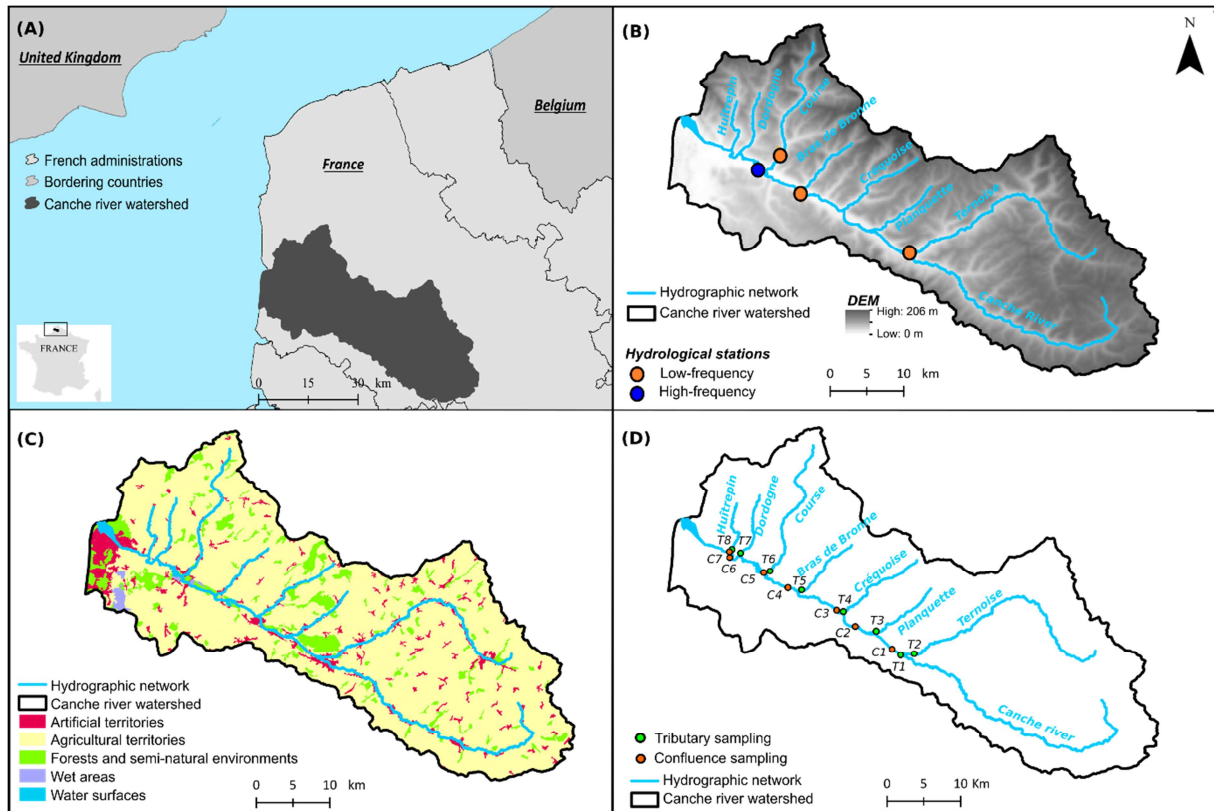


Figure 1 : (A) Overview of the Canche river watershed, (B) Digital elevation model (DEM; m), hydrographic network and location of monitoring stations, (C) Corine Land Cover 2012 and (D) Location of sediment sampling for the study.

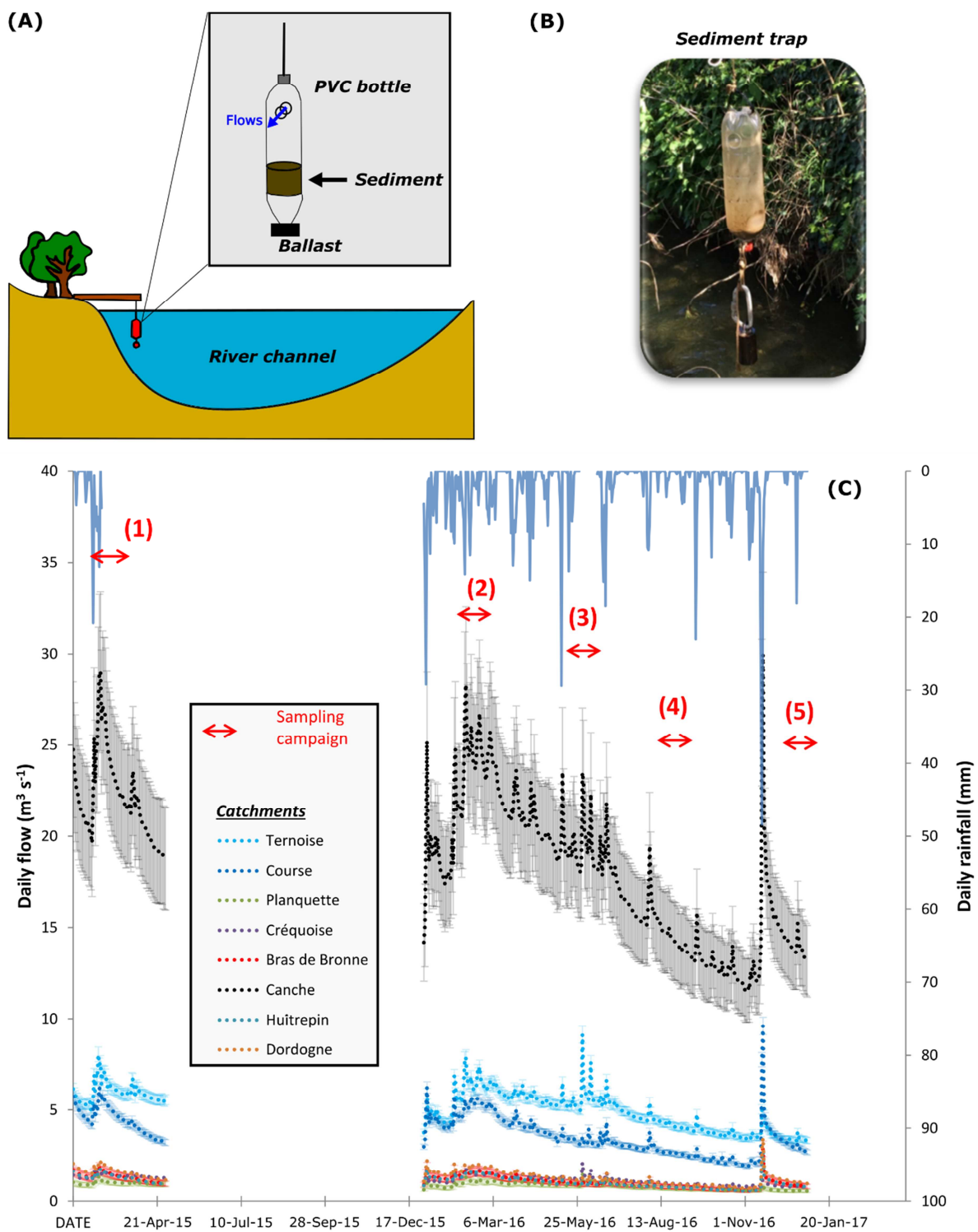


Figure 2 : (A, B) Protocol and experimental device used to sample suspended particulate matter (SPM) for each tributary and confluence in the study, (C) temporal variability of the flow discharge in the Canche river watershed during the five seasonal sampling campaign.

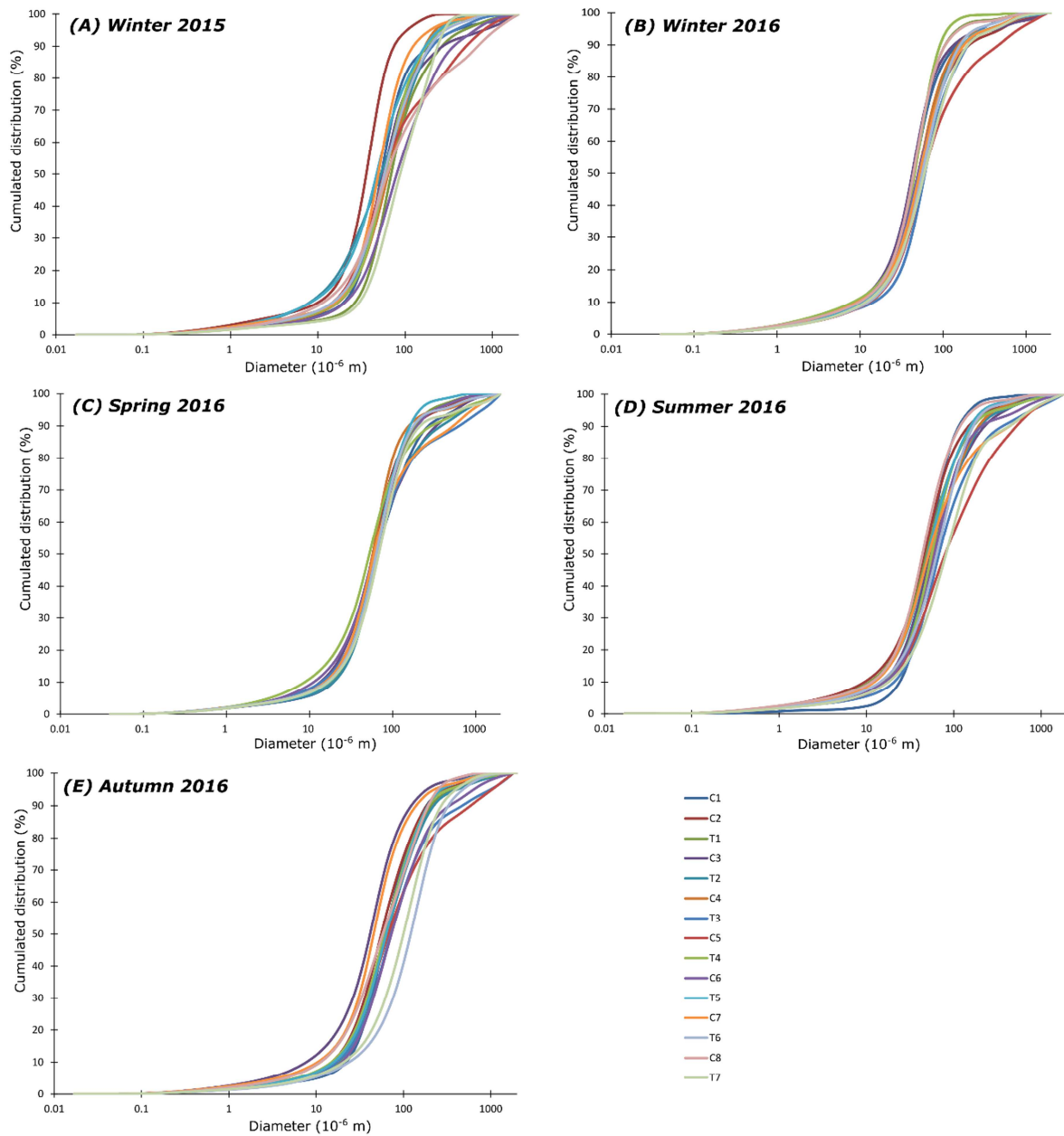


Figure 3: Grain size distribution for all samples collected in the Canche river watershed.

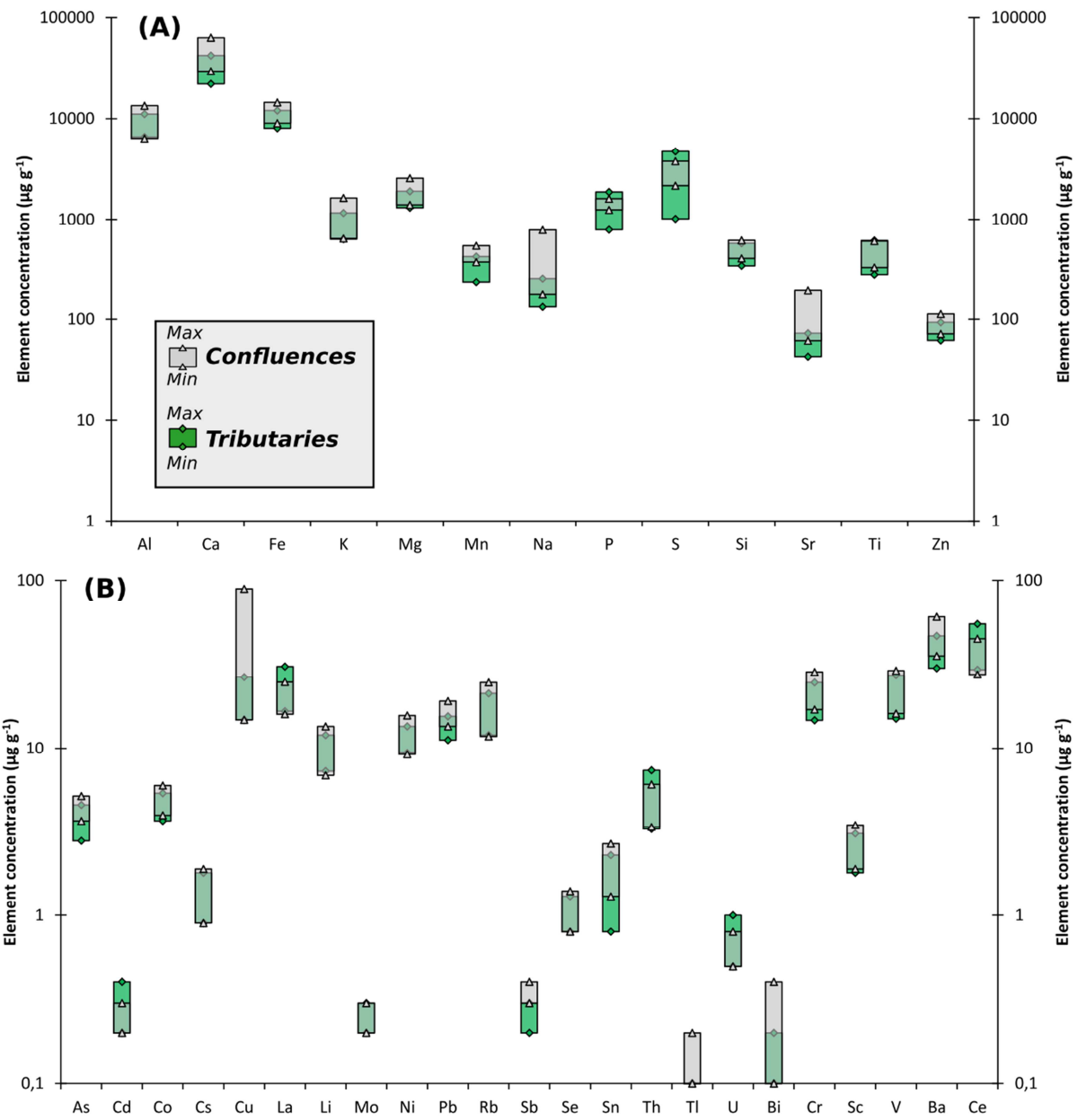


Figure 4: Range of concentrations (expressed in $\mu\text{g g}^{-1}$) of major elements (A) and trace elements (B) in the sediment trap samples during the five seasonal sampling campaigns.

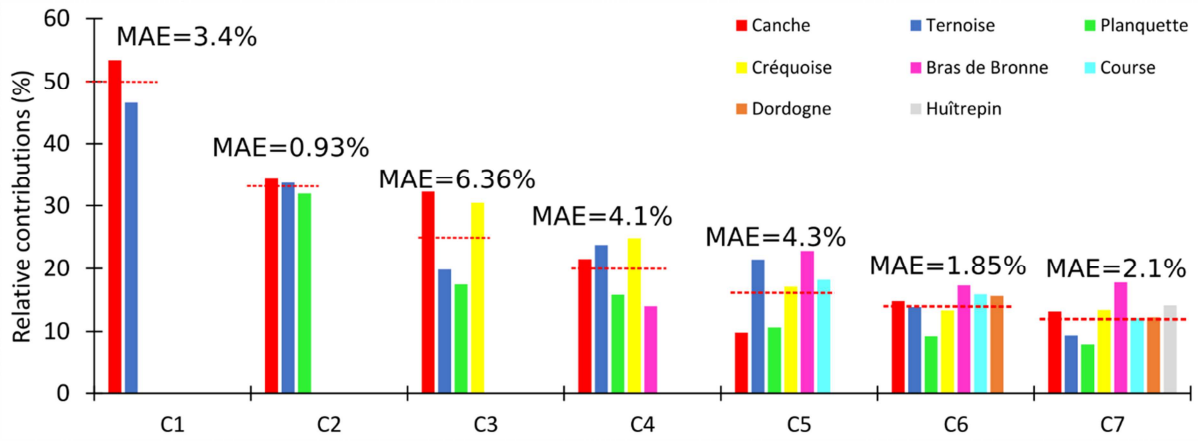


Figure 5 : Mixing model results using virtual mixtures, at each confluences. Red dotted lines indicates the hypothetical contributions (e.g. equal inputs from each tributary). MAE refers to the Mean Absolute Error (%).

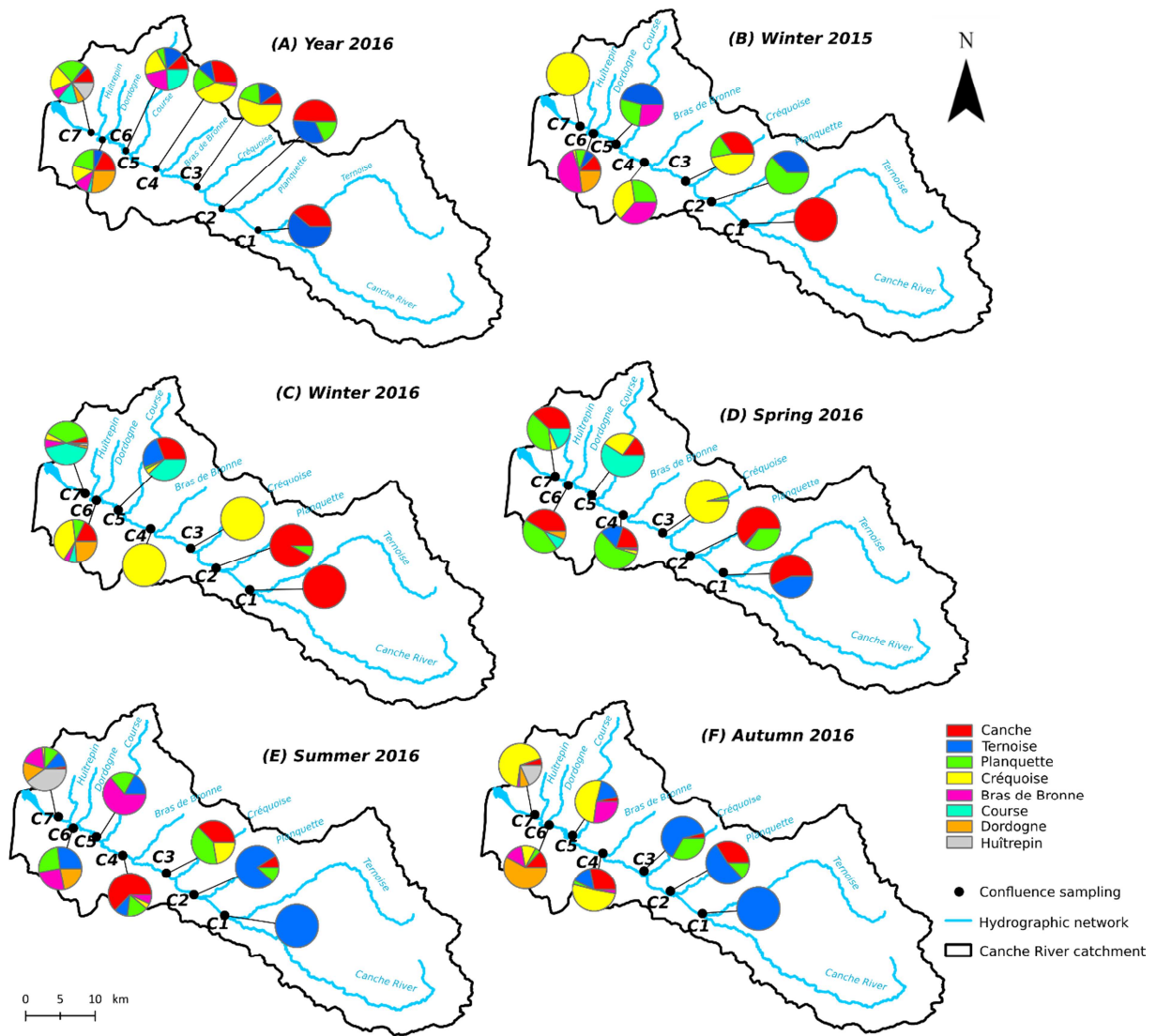


Figure 6 : (A) Annual tributaries relative contributions (%) to the sediment yield in the Canche river watershed and, (B, C, D, E, F) seasonal tributaries relative contributions (%) to the sediment yield in the Canche river watershed.

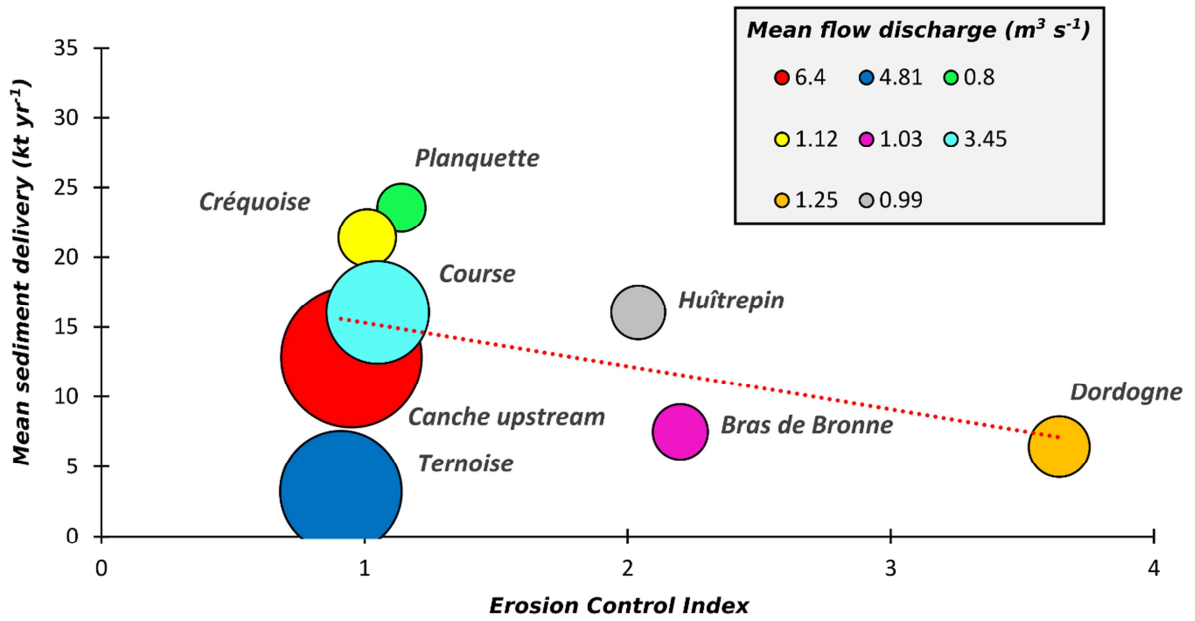


Figure 7: Evaluation of each tributary sediment delivery ($kt yr^{-1}$) as a function of the Erosion Control Index (number of erosion control measures per km^2). The bubbles indicates the annual mean flow discharge ($m^3 s^{-1}$). The red dotted line indicates the trend ($R = 0.41$).

Tables

Tab. 1: Results of the Bracket test to determine conservative tracers at each confluence.

Confluence	Conservative tracers
C1	As, Co, La, Mo, Ni, Sn, Th, U, Ce, Al, Ca, Fe, K, Mg, Na, P, S, Sr, Ti, Zn
C2	Cd, La, Sn, Th, U, Ce, Na, Si, Ti
C3	As, Co, Cu, La, Mo, Pb, Sb, Se, Sn, Th, Tl, U, Bi, Cr, V, Ba, Ce, K, Mg, Mn, Na, Si, Sr, Ti, Zn
C4	As, Cd, Co, Cs, La, Li, Pb, Rb, Sb, Sn, Th, Tl, U, Bi, Cr, Sc, V, Ba, Ce, Al, Ca, Fe, K, Mg, Mn, Na, P, S, Si, Sr, Ti, Zn
C5	As, Cd, Co, Cs, Cu, La, Ni, Pb, Rb, Sb, Se, Sn, Th, U, Ba, Ce, Al, Ca, Fe, Mg, Mn, Na, P, S, Si, Sr, Ti, Zn
C6	As, Cd, Co, Cs, Cu, La, Li, Mo, Ni, Pb, Rb, Sb, Se, Sn, Th, Tl, U, Bi, Cr, Sc, V, Ba, Ce, Al, Fe, K, Mn, P, S, Si, Ti, Zn
C7	As, Cd, Co, Cs, La, Li, Mo, Ni, Pb, Rb, Sb, Se, Sn, Th, U, Bi, Cr, V, Ba, Ce, Al, Fe, Mn, P, S, Si, Ti, Zn

Tab. 2: Results of the stepwise DFA to identify the final composite fingerprint at each confluence.

C1			C2			C3			C4			C5			C6			C7		
Tracer	% ^a	TDW ^b	Tracer	% ^a	TDW ^b	Tracer	% ^a	TDW ^b	Tracer	% ^a	TDW ^b	Tracer	% ^a	TDW ^b	Tracer	% ^a	TDW ^b	Tracer	% ^a	TDW ^b
Co	60	1.5	La	47	3.5	Bi	44	2.3	Ca	36	3	Ca	34	8.1	Mo	13	2	Mo	14	2.6
Ni	50	1.3	U	40	3	Sr	20	1.1	Bi	30	2.5	Mn	16	3.7	Pb	26	4	Pb	23	4.1
Mg	60	1.5	Na	13	1	Sb	19	1	Mn	19	1.6	Mg	15	3.5	As	16	2.4	As	9	1.6
Ca	40	1	Ti	20	1.5	As	23	1.2	Si	23	1.9	Sb	13	2.9	Se	7	1.1	Se	6	1.1

Total ^c	100	Cd	47	3.5	Se	20	1.1	K	12	1	Si	17	3.9	Ni	6	1	Co	8	1.3
		Si	13	1	Ti	34	1.8	Sb	15	1.3	Cs	13	2.9	Fe	27	4.2	Ni	9	1.6
		Total ^c	53		Total ^c	85		Fe	24	2	Rb	8	1.9	Co	11	1.7	Fe	21	3.8
								Total ^c	69		Sr	14	3.3	P	7	1.1	Mn	12	2.1
											Na	4	1	Mn	14	2.1	Zn	8	1.3
											P	8	1.9	Zn	9	1.3	Cs	9	1.7
											As	12	2.7	Total ^c	54		Al	11	1.9
											Ni	8	1.7				Cd	6	1
											Cd	8	1.7				Cr	18	3.1
											Total ^c	62					Total ^c	58	

^a % source type samples correctly classified by the tracer.

^b tracer discriminatory weighting used in the mass balance modelling.

^c % source type samples classified correctly by the final composite fingerprint.

Graphical abstract

